COMBINING S-SPACE AND IMAGE SPATIAL INFORMATION FOR CHARACTERIZATION OF LAND-COVER ELEMENTS USING AVIRIS DATA

Conrad M. Bielski
NASA JPL, 4800 Oak Grove Dr., Pasadena, CA, 91109
conrad.m.bielski@jpl.nasa.gov

Abstract: Imaging spectroscopy data provides information that is both spatially and spectrally rich. However, hyperspectral classification and identification procedures are generally based solely on the spectral data. The S-space concept treats the spectrum as a 'spatial' dimension thereby facilitating the exploration of a relationship between the spectral and spatial image domains. This paper presents the ideas that will be researched as well as some preliminary results.

1.Introduction

Imaging spectroscopy data is becoming more available to the remote sensing community due to the increased number of sensors put into commission over the last few years. This is favourable news for the land-cover community because the increase in potential information that can be obtain from such data is promising. However, the tools currently available are generally based solely on the spectral signature even though the spatial content can provide a significant amount of information. A reason for not combining the two types of data into the information extraction process is due to the unknown relationship between the spatial and spectral dimensions. For example, the standardized AVIRIS Processing Methodology (Kruse, 1999) proposes calculation of the Pixel Purity Index and N-dimensional Visualization for endmember definition. All of which are solely based on the spectral signature at each measured location.

This paper introduces the ideas that were put forth for post-doctoral research with the AVIRIS lab at the Jet Propulsion Laboratory. These ideas were based on the observation that a spectral signature resembles quite closely many other spatial type measurements. Even though the Electromagnetic (EM) spectrum itself is not considered as a spatial domain, this similarity to the spatial dimension could be explored and more easily associated to the spatial dimension. A first attempt at examining the spectral variability of imaging spectrometer data using Geostatistical tools is presented. Geostatistics is concerned with the study of phenomena that fluctuate in space (Olea 1991) and has been widely applied in the remote sensing context to understand and model the spatial variability inherent in remote sensing scenes. One example is Curran and Dungan's (1989) work on estimating the per-band signal-to-noise ratio in AVIRIS data using the semivariogram model nugget information.

Four sections make up the remainder of this paper. Section 2 introduces the S-space concept followed by a section dedicated to describing the quantification of the spectra using the semivariogram. The next section presents examples and preliminary results based on AVIRIS imaging spectrometer data. The final section describes some ideas and future work.

2.Spectral space or S-space

As mentioned above, the spectral signature recorded by an imaging spectrometer very closely resembles other types of spatial measurement. In figure 1, a comparison was made between a measure of soil pH along a transect (figure 1, left side) and a hypothetical measure of radiance or reflectance taken at different wavelengths (figure 1, right side). Envisioning the spectral signature in this manner gives one the spatial sense of the EM spectrum. Furthermore, the idea that measured point B is closer to point A then point C reinforces this idea of 'spatial distance'. In order not to confuse this type of space with spectral space which can also mean spectral feature space, S-space was coined in order to differentiate the two (Bielski et al. 2002). The spatial measures in S-space are wavelengths or frequency. Since S-space is one dimensional, distance between measurements are analogous to the difference in wavelength or frequency.

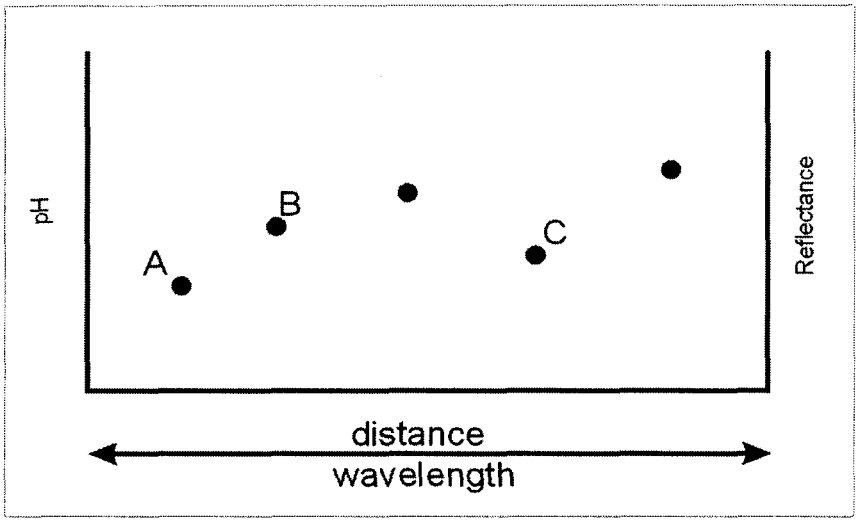

Figure 1 – S-space illustration: a theoretical profile was compared with a sampling transect in order to show similarities between geographical space and S-space. Point A is closer to point B both in S-space and geographical space when compared with point C.

3.Quantifying Spectral Variability

The variability in S-space was computed using the variogram, a Geostatistical tool. Previous work has demonstrated the applicability of the semivariogram for the quantification of the spatial variability inherent in remotely sensed imagery (Curran 1988, Woodcock et al. 1988a, b, Jupp et al. 1988). The experimental semivariogram is a univariate statistic that measures the average dissimilarity between data separated by a lag h. The lag in S-space was considered to be the spectral distance between image bands. Mathematically, the semivariogram is computed as half the average squared difference between the components of every data pair:

$$\gamma(\mathbf{h}) = \frac{1}{2N(\mathbf{h})} \sum_{i=1}^{N(\mathbf{h})} [z(u_\alpha) - z(u_\alpha + \mathbf{h})]$$

where z is the radiance or reflectance at the spectral space location u, and N(h) is the number of data pairs at a spectral distance h apart. In the two dimensional case, location pairs are found by jumping the necessary h pixels apart for each lag (figure 2). Since the spectral signature is one dimensional, the semivariogram is computed along a transect as in figure 2. This method of computing the S-space semivariogram was used as a means of generating initial results even though in reality imaging spectroscopy data does not necessarily provide equidistant bandwidths. The bandwidths making up AVIRIS imagery are not equidistant and should therefore be taken into account in the computation of the experimental semivariogram.

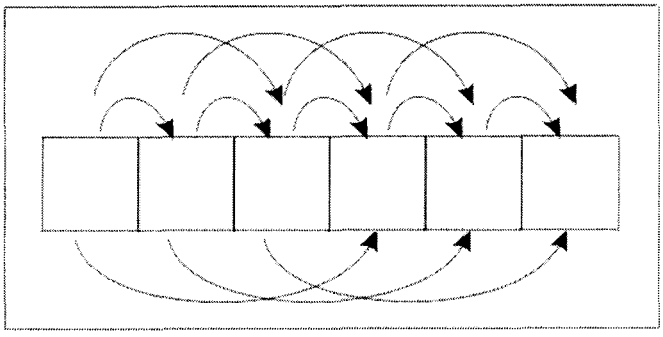

Figure 2 – Computing the experimental semivariogram along a transect of pixels. Each arrow designates a different size h. In S-space, the varying bandwidth must be taken into account.

Computing the experimental semivariogram is but the first step. Since the data acquired by the sensor does not have infinitely small distances between samples, the second step is to fit a mathematical model to the experimental model. The modeled semivariogram will then have variance values for any lag h which is necessary for solving interpolation equations (e.g. kriging). Another reason for modeling the experimental semivariogram was to diminish the number of resulting bands even further. A modeled semivariogram (single model) is made up of three parameters: the nugget, sill and range (figure 3). The nugget is a description of the unknown variability between the smallest sampling interval. The sill is the plateau of the variance and the range is the distance at which the sill is attained.

The expected shape of a typical semivariogram is that variances at shorter lags are smaller because objects that are closer together tend to be more similar. As the distance increases between pairs of points, objects become less similar thereby increasing the variance. A horizontal semivariogram indicates no spatial variability because the variance of close data pairs is the same as with data pairs further apart.

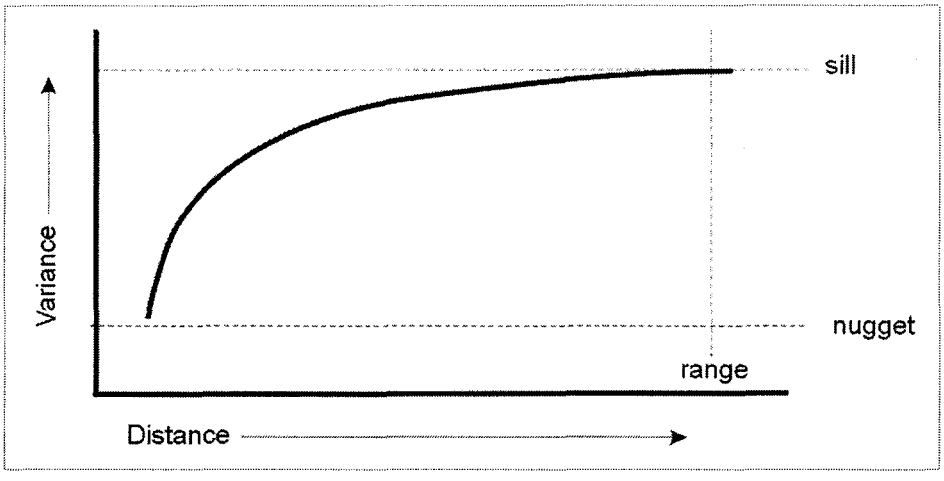

Figure 3 – The ideal semivariogram. Three parameters modeling a single model semivariogram: the nugget, sill and range.

4.Results of Initial Experiments

This section presents results of computing the experimental semivariogram on AVIRIS imagery. The image is of an experimental agricultural field in the Salinas Valley region of California acquired on October 9, 1998 (figure 4). The image shows rows of broccoli at different stages of growth as well as lettuce and senescent corn. The perfect rows of planted vegetation were easily discerned and also have a distinct spatial pattern that was easily observed in the computed experimental variogram.

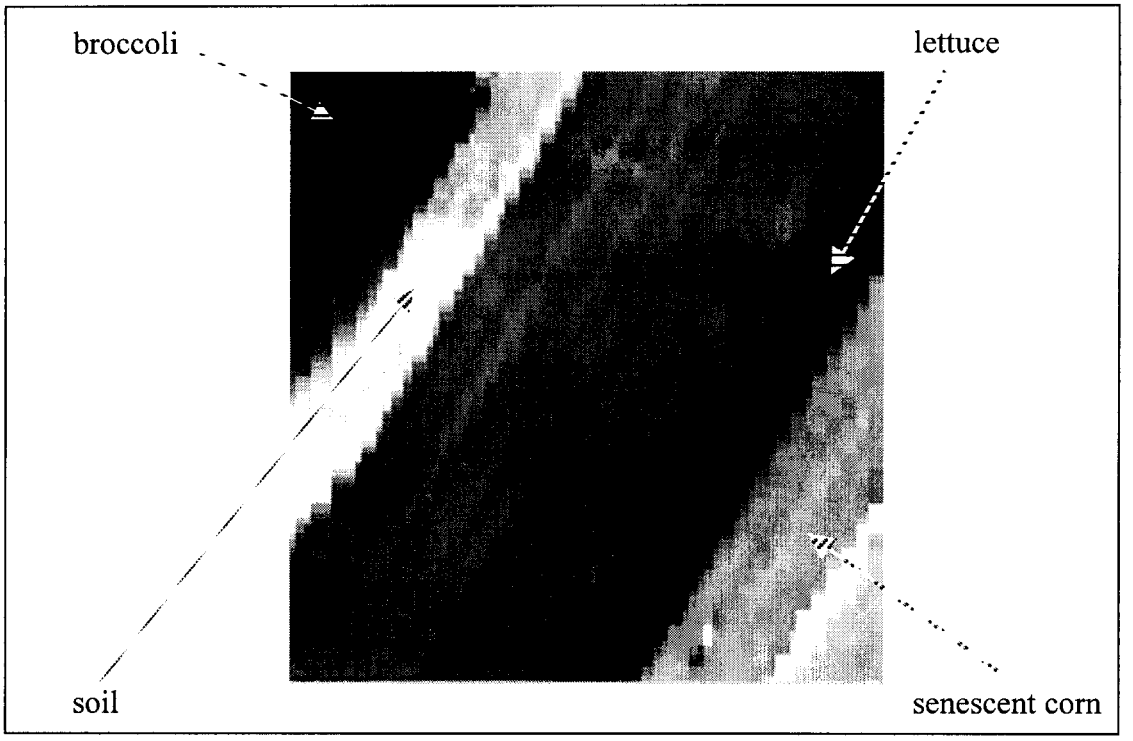

Figure 4 – AVIRIS image of Salinas Valley agricultural field taken October 9, 1998. Shown are mature broccoli, bare soil, senescent corn and lettuce.

A set of two dimensional semivariograms was computed on ten bands of the AVIRIS data set. The first semivariograms were computed for band 20 and then for every 20th band after that. Three directional semivariograms were computed from top/bottom, at a 45° angle and side/side. The results are shown in figure 5 and presented an interesting view of how the bands differed spatially. The close resemblance between the top/bottom and 45° angle semivariograms was due to the fact that the rows do not exactly run at a 45° angle and therefore had a similar spatial variability as the top/bottom semivariogram. The side/side semivariogram (figure 5, right side) showed that a sill was reached and then the pixel pairs began to resemble each other again at increasing lags. This was most likely due to the fact that the most mature vegetables were found at the sides of the image where the largest lags would reach.

The one band that had the same semivariogram shape across all three plots was band 160. This band continuously produced an almost horizontal plot in all three cases. As mentioned previously, this occurs when there is a lack of quantifiable spatial variability. It turns out that the AVIRIS band number 160 was within a water vapour absorption band.

Figure 6 presents the actual images from which each of the above semivariograms were computed. The bands with the well defined semivariograms did have an obvious spatial component. However, band 160 did not and this resulted in a horizontal experimental semivariogram.

The images in figure 6 also showed the variability inherent spectrally for each of the row crops. It is precisely this variability that needs to be harnessed and related to the spatial dimension.

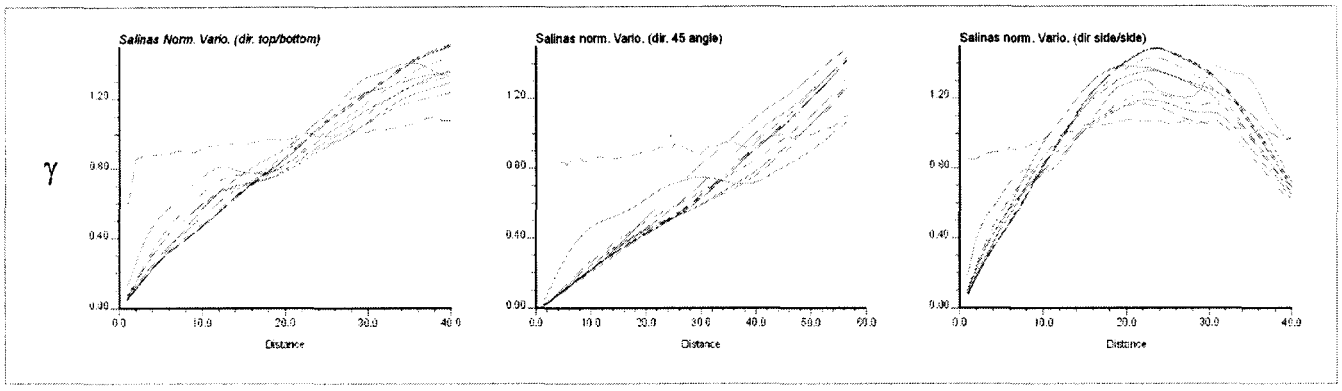

Figure 5 – Computed semivariogram in three directions: top/bottom (left), 45° angle (center) and side/side (right) for 10 AVIRIS spectral bands.

Band 20 – red	Band 120 – blue stripe
Band 40 – red stripe	Band 140 – violet
Band 60 – green	Band 160 – violet stripe
Band 80 – green stripe	Band 180 – black
Band 100 – blue	Band 200 – black stripe

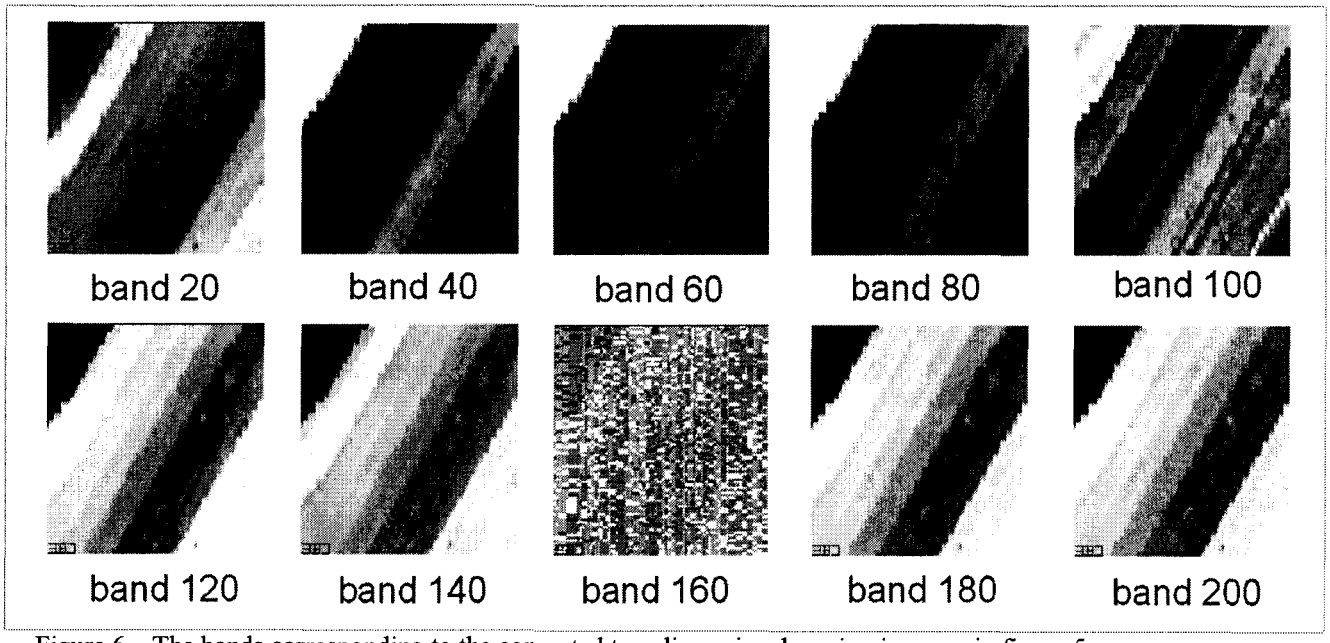

Figure 6 – The bands corresponding to the computed two dimensional semivariograms in figure 5.

S-space was first explored with a simple computation of the average spatial variability across the entire Salinas image. Specifically, the experimental semivariogram was computed in the z-direction (i.e. along the spectrum) and averaged across all the pixels within the image. This resulted in a single plot (figure 7). A quick analysis of the computed semivariogram over the entire spectrum recorded by AVIRIS showed that as the distance between bands increased so did the S-space variability. This first analysis also showed that there was spatial variability in S-space. Upon closer examination, three distinct features were observed. A nugget effect was present but very small and around lag 20 a small but evident plateau was observed which indicated small scale variability between lags 0 and 20. A second plateau was observed between lags 40 to 45 which indicated a second scale of S-space variability.

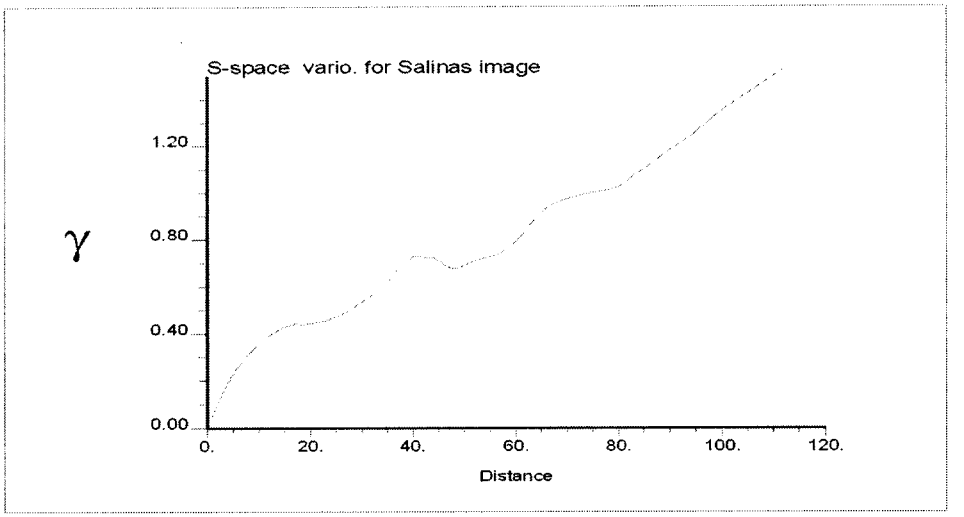

Figure 7 – The semivariogram computed in S-space (z-direction) for the Salinas Valley image.

Averaging all the spectral signatures over the entire image lost many details. Subsequently, four pixels were chosen from different land-covers for a more detailed look at the S-space variability. A single pixel from each of mature broccoli, bare soil, senescent corn and lettuce were chosen. Their spectral signatures are presented in figure 8. The S-space experimental semivariogram was computed based on these four spectral signatures (figure 9, top). The first observation noted the very high variance for all of the computed semivariograms. This was due to the fact that radiance measures were used in the computation. Another interesting result was the relationship between the S-space variability and the resulting experimental semivariogram. Those spectral signatures with large variations produced the highest sills, i.e. broccoli and lettuce. The lower plot in figure 9 showed the normalized semivariograms. The shapes of these semivariograms were more defined with broccoli and lettuce having larger bumps than the senescent corn and soil.

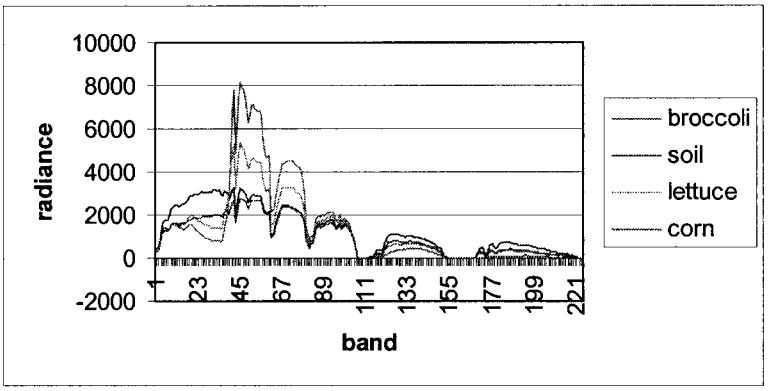

Figure 8 – Four pixels representing mature broccoli (orange), bare soil (pink), senescent corn (green) and lettuce (blue) and their associated spectral signature (left plot).

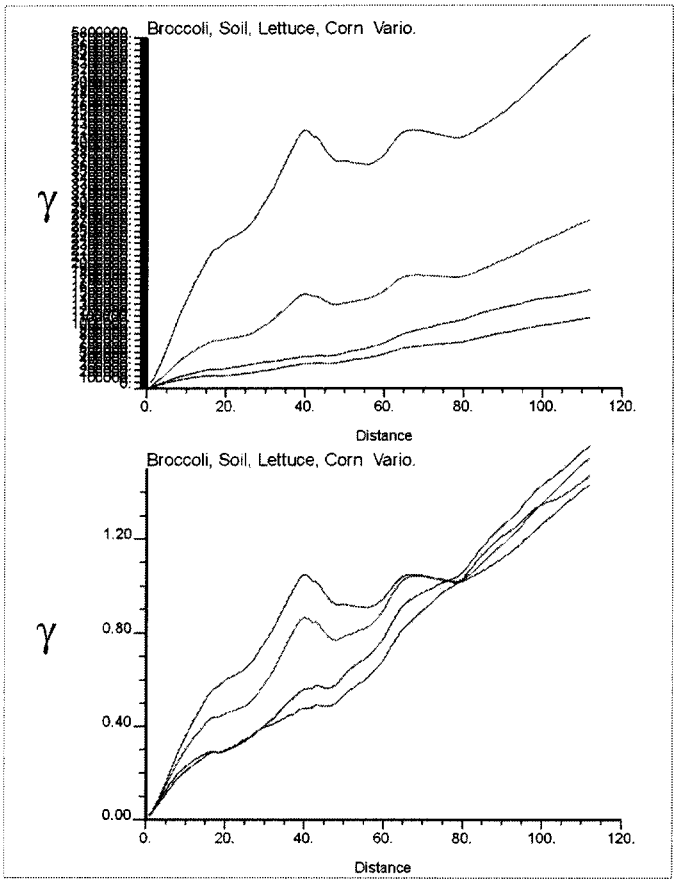

Figure 9 – Computed experimental semivariogram (top) and normalized experimental semivariogram (bottom) based on the four spectral signatures in figure 8.

5.Future Directions

The above results were preliminary and served to provide an insight into the use of Geostatistical tools to S-space. An important result was the fact that the spectral signatures did in fact have quantifiable spatial variability. This fact alone is interesting enough to continue the investigation further. One possible use of modeling the spatial variation is to interpolate the spectral signature in areas where there is no data available or the data has been corrupted.

Ultimately, the direction of this research is to study the relationship between the spectral component of remotely sensed imagery and that of the spatial component. While both are distinct, they are the most important components making up a remotely sensed image for information extraction purposes. Combining the two types of information should increase the performance of automatic classification algorithms.

6.References

Bielski, C. M., Dubé, P., Cavayas, F., and Marceau, D. J., 2002, S-space: a new concept for information extraction from imaging spectrometer data. International Journal of Remote Sensing, 23(10), 2005-2022.

Curran, P.J., 1988, The semi-variogram in remote sensing: an introduction. Remote Sensing of Environment, 37, 493-507.

Curran, P.J., and Dungan, J.L., 1989, Estimation of signal to noise: a new procedure applied to AVIRIS data. IEEE Transactions of Geoscience and Remote Sensing, 27, 620-628.

Jupp, D. L. B., Strahler, A. H., and Woodcock, C. E., 1988, Autocorrelation and regularization in digital images: I. Basic Theory. IEEE Transactions on Geoscience and Remote Sensing, 26, 463-473.

Kruse, F.A., 1999, Visible-Infrared Sensors and Case Studies. Chapter 11 in Manual of Remote Sensing, Third Edition, Volume 3, Remote Sensing for the Earth Sciences, Andrew N. Rencz editor. John Wiley & Sons, Inc.

Olea, R. (ed.), 1991, Geostatistical Glossary and Multilingual Dictionary (New York: Oxford University Press).

Woodcock, C. E., Strahler, A. H., and Jupp, D. L. B., 1988a, The use of variograms in remote sensing: I. Scene models and simulated images. Remote Sensing of Environment, 25, 323-348.

Woodcock, C. E., Strahler, A. H., and Jupp, D. L. B., 1988b, The use of variogram in remote sensing: II. Real digital images. Remote Sensing of Environment, 25, 349-379.